Hindawi Publishing Corporation
Journal of Chemistry
Volume 2013, Article ID 617498, 6 pages
http://dx.doi.org/10.1155/2013/617498

Research Article

Synthesis of Poly(cyclohexene oxide)-Montmorillonite Nanocomposite via *In Situ* Photoinitiated Cationic Polymerization with Bifunctional Clay

Işıl Bayram,[1] Ayhan Oral,[1] and Kamil Şirin[2]

[1] *Department of Chemistry, Faculty of Arts and Science, Çanakkale Onsekiz Mart University, 17020 Çanakkale, Turkey*
[2] *Department of Chemistry, Faculty of Arts and Sciences, Celal Bayar University, Campus of Muradiye, 45030 Manisa, Turkey*

Correspondence should be addressed to Ayhan Oral; ayhanoral@comu.edu.tr and Kamil Şirin; kamil.sirin@cbu.edu.tr

Received 26 March 2013; Accepted 28 May 2013

Academic Editor: Marinos Pitsikalis

Copyright © 2013 Işıl Bayram et al. This is an open access article distributed under the Creative Commons Attribution License, which permits unrestricted use, distribution, and reproduction in any medium, provided the original work is properly cited.

Poly(cyclohexene oxide) (PCHO)/clay nanocomposites were prepared by means of *in situ photoinitiated cationic polymerization* with initiator moieties immobilized within the silicate galleries of the clay particles. Diphenyliodonium molecules were intercalated via cation exchange process between Cloisite Ca and diphenyliodonium. The polymerization of CHO through the interlayer galleries of the clay can provide a homogenous distribution of the clay layers in the polymer matrix in nanosize and results in the formation of PCHO/clay nanocomposites. The rates of clay loadings were changed to 1%, 3%, and 5% so as to investigate the effect of clay and initiator amount on polymer. X-ray diffraction (XRD) spectroscopy, thermogravimetric analysis (TGA), and transmission electron microscopy (TEM) methods were used for the characterization of modified clay and nanocomposite materials. Thermal stability of PCHO/MMT nanocomposites was also studied by both differential scanning calorimetry (DSC) and thermogravimetric analysis (TGA).

1. Introduction

Polymer/layered silicate nanocomposites have attracted a great interest thanks to their excellent performances when compared with conventional composites. The use of inorganic particle-filled composites can improve not only the physical properties of the materials but also the mechanical properties, the thermal resistance, the gas barrier, and the chemical reagent resistance and can also provide high-performance materials at a lower cost [1–5].

Three methods have been utilized for the preparation of the polymer-clay nanocomposites, which are solution intercalation, melt intercalation, and *in situ* polymerization [6]. The properties of the polymer/layered silicate nanocomposites depend on the distribution and dispersion of the layered silicate in the polymer matrix. The main aim of these preparation methods is to obtain the best distribution of the clays in the polymer matrix and a strong polymer-clay interaction. The first two methods have several disadvantages. These include the requirement of a large amount of solvent and slow transportation of the polymer into the interlayer space. These limitations are overcomed by using *in situ* polymerization method and clay/polymer nanocomposites with high homogeneity. When organoclay is swollen within a monomer and initiating species are generated by external stimulation of reactive groups attached to the surface, it can lead to the formation of polymer between the intercalated sheets. Thus, the nature of the polymerization is expected to play an important role in the exfoliation process [7]. *In situ* polymerization method is an effective method to obtain best distribution [8].

However, photopolymerization has been scarcely applied to the preparation of polymer/montmorillonite clay nanocomposites. The use of UV-curing process is becoming widespread in micro- and consumer electronics industries due to their rapid cure, solvent free characteristics, application versatility, low energy requirements, and low temperature operation [9]. The UV-curing technique [10] can be suitable to perform *in situ* intercalative polymerization to obtain nanocomposites. The clays can be dispersed in the liquid monomers and upon irradiation polymeric matrix and can be built

through a fast process, without using solvents and heating the system. In this case, a cationic mechanism occurs, and the process is not sensible to oxygen (which means that there is no need of an inert atmosphere). Although most of the technically applied photopolymerizations are based on free radical polymerization, photoinitiated cationic polymerization has become attractive after the discovery of iodonium and sulfonium salts [11]. These salts typically decompose to yield protons when irradiated at their higher absorption wavelength.

Initiation process is an important step to prepare nanocomposite preparation. We are the first to report the use of diphenyliodonium-loaded clay both as an initiator and inorganic filler for preparation of PCHO/clay nanocomposite via *in situ* photoinitiated polymerization. In this case, actual propagation begins in interlayer space of the clay platelets. Thus, the clay platelets are homogenously distributed in the polymer matrix leading to the formation of exfoliated poly(cyclohexene oxide) (PCHO)/clay nanocomposites. The method consists of two steps: the loading of catalyst via cation exchange process of diphenyliodonium, followed by *in situ* photopolymerization of CHO in the presence of catalyst loaded clay. The characterization of the nanocomposites products was carried out by TGA, X-ray diffraction (XRD), and TEM.

2. Materials and Methods

2.1. Materials. Cloisite Ca (Southern Clay products, Gonzales, TX, USA). Cyclohexene oxide (CHO, Aldrich, 98%) was vacuum-distilled from calcium hydride before use. Lithium chloride (LiCl, Fluka 98%), diphenyliodonium hexafluorophosphate ($DPI^+PF_6^-$, Fluka 98%) were used as received. Dichloromethane (DCM, Acros, HPLC grade) was stored on calcium hydride and used after distillation. Other solvents were purified by conventional drying and distillation procedures.

2.2. Characterization. Various characterization techniques were used in order to describe the cation exchanged amount of the diphenyliodonium to evaluate the dispersion of the nanoclay in the polymer matrix and to investigate the effect of the clay on polymer properties, X-ray diffraction (XRD) spectroscopy, thermogravimetric analysis (TGA), and transmission electron microscopy (TEM) methods were used for the characterization of modified clay and nanocomposite materials. Thermal stability and glass transition temperatures of PCHO/MMT nanocomposites were also studied by thermogravimetric analysis (TGA) and differential scanning calorimetry (DSC).

2.2.1. Molecular Weight. Gel permeation chromatography (GPC) measurements were obtained from an Agilent Model 1100 consisting of a pump, a refractive index detector, and four Waters Styragel columns as HR 5E, HR 4E, HR 3, and HR 2, and THF was used as an eluent at a flow rate of 1 mL/min at 30°C. Molecular weights were calibrated using polystyrene standards. Before the GPC measurements, the nanocomposite in THF solution of lithium chloride was refluxed for about 24 h to cleave the polymer from clay. After the refluxing centrifugation process, the polymer was precipitated in methanol.

2.2.2. Thermal Analysis. Thermal gravimetric analysis (TGA) evaluation of the neat polymer and hybrids was performed via Perkin-Elmer Diamond TA/TGA. Instruments were warmed up with a heating rate of 10°C min under nitrogen (flow rate: 100 mL min^{-1}) up to 700°C. This method was used both to determine the amount of the modificators which penetrated intergalleries of the clay and to investigate thermal stability of the products.

Glass transition (T_g) of pristine polymer and nanocomposites was determined using a differential scanning calorimeter (DSC), TA2920, TA instruments, operated at a heating rate of 5°C/min.

2.2.3. XRD Pattern. To evaluate the dispersion of the nanoclay in the polymer matrix, XRD measurements were performed at room temperature with a Siemens D5000 h/h diffractometer equipped with an intrinsic germanium detector system with Cu Kα radiation (λ: 1.5406 Å).

2.2.4. Transmission Electron Microscopy. Transmission electron microscopy (TEM) images were obtained from Philips-FEI Tecnai G2 F20 S-Twin 200 kV accelerating voltage. The samples have been dispersed in THF, and then some drops were deposed on a grid. After solvent evaporation, the TEM micrograph analyses were performed. Distribution of the clay platelets in the polymer matrix and particle size of the filler in the polymer matrix were evaluated via this method.

2.3. Modification of Clay. The initiator loading was carried out according to ion-exchange process (Figure 1). For this purpose, 1.0 g of Cloisite-Ca was dispersed into 50 mL DCM at room temperature, and the suspension was stirred for 30 min. A 1 g sample of the DPI was added into the Cloisite-Ca.

DCM dispersion was stirred under vigorous stirring. Stirring was continued for 24 hours in the dark. The exchanged clay was centrifuged and washed twice with DCM to remove adsorbed molecules. It was then dried in vacuum at room temperature. The organophilic MMT was obtained through a multistep route and donated D-MMT. Before use, the clay was dried under vacuum at 110°C for 1 h.

2.4. Preparation of the PCHO/Clay Nanocomposites. The D-MMT (2.1×10^{-5} mol initiator for 1% loading) was mixed with CHO (2 mL, 2000×10^{-5} mol) monomer and DCM (2 mL) in quartz tubes via a magnetic stirrer at room temperature and degassed with nitrogen before irradiation by a merry-go-round type reactor equipped with 16 Philips 8 W/06 lamps emitting light nominally at 300 nm and a cooling system. The light intensity at the location of the polymerization tube was measured by a Delta Ohm model HD-9021 radiometer.

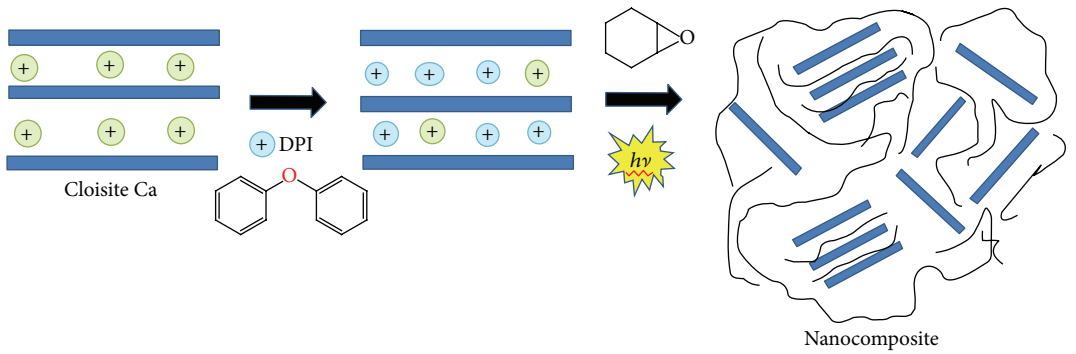

Figure 1: Cation exchange and nanocomposite preparation. Cloisite-Ca: Cloisite Calcium, DPI: diphenyliodonium, *hv*: UV Light, Nanocomposite: Poly(Cyclohexene oxide)-Montmorillonite nanocomposite structure.

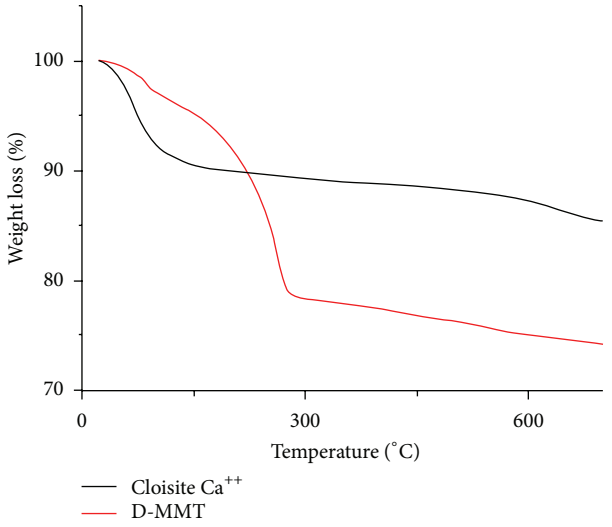

Figure 2: TGA diagram of Cloisite-Ca and D-MMT.

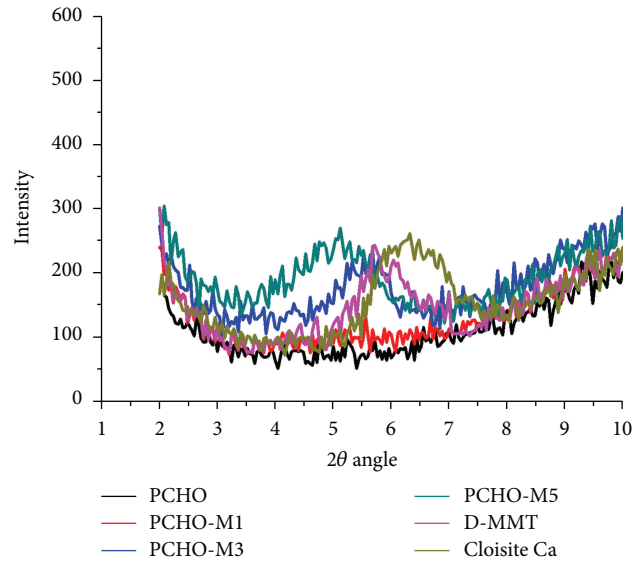

Figure 3: X-ray diffractions of Cloisite Ca, D-MMT, pristine polymer, and clay-loaded nanocomposites.

After the 4 h irradiation, polymers were dissolved in DCM, precipitated into methanol, filtered, dried, and weighed.

A series of polymerizations were carried out using various D-MMT loadings (1, 3, and 5% of the monomer by weight) by following the same steps.

3. Results and Discussion

TGA was used both to determine organic content of the diphenyliodonium-modified montmorillonite and to investigate the effect of clay loadings on thermal stability of the polymer.

Diphenyliodonium exchanged MMT was identified via TGA. According to TGA diagrams (Figure 2), the amount of immobilized initiator was determined via TGA to be 60 mequiv/100 g immobilized initiator per g clay. This value is lower than that for the case of complete ion exchange because CEC values for smectic clays are reported to range from 60 to 120 mequiv/100 g [12, 13]. This smaller CEC value is attributed to the greater sterical demands of the initiator (diphenyliodonium) when compared with smaller inorganic ions (Ca^{2+}).

The first step of mechanism for the cationic polymerization of epoxides is initiation by both radical cation and cation. Cationic groups were generated photochemically upon photolysis of cationic photoinitiators such as onium salts. The resulting cationic species react with the monomer or impurities in the reaction mixture to generate protonic acids. These acidic parts initiate cationic polymerization of the epoxides.

The level of intercalation/exfoliation was characterized by XRD.

After the clay was modified with diphenyliodonium, it both showed improved compatibility with the polymer matrix, and polymerization process was initiated via diphenyliodonium that was situated in the intergalleries of the clay. Such an exfoliation is more likely to arise from growing PCHO chains interlayer galleries of the clay for lower clay loading, which pushes the platelets away from each other and stabilizes each layer individually. Thus, the clay galleries could be easily exfoliated with the polymer. The disappearing of a diffraction peak at low 2θ angles suggests the formation of an exfoliated structure. For the PCHO hybrids with 3 and 5 wt% organoclay, obvious clay peaks appeared in their XRD curves in Figure 3. This indicated that these organoclay layers were not entirely exfoliated and were not homogeneously

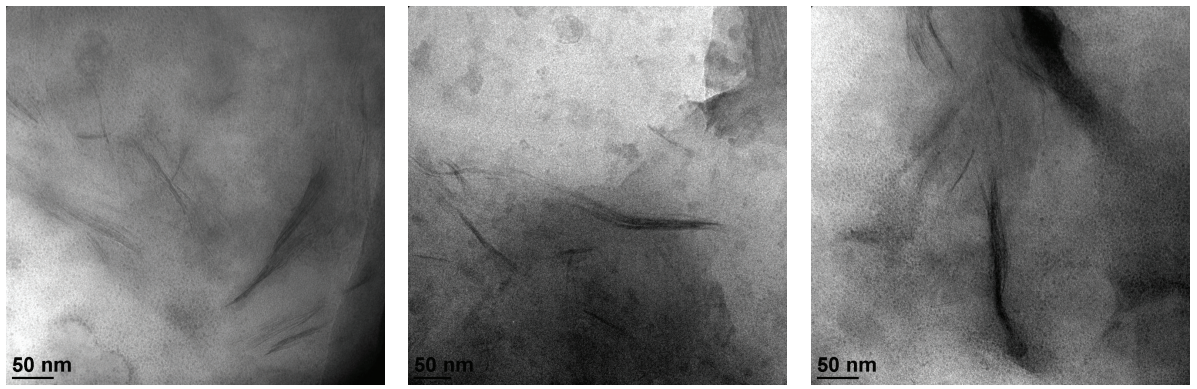

Figure 4: TEM micrographs of PCHO/clay nanocomposites, PCHO/M1, PCHO/M3, and PCHO/M5.

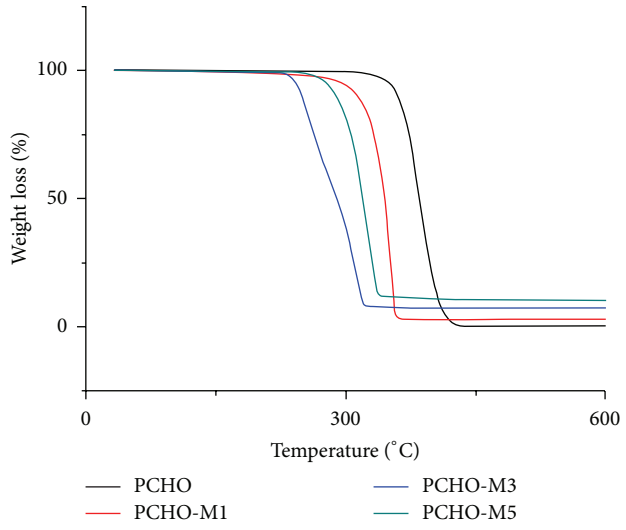

Figure 5: TGA diagram of pure polymer and nanocomposites.

dispersed in the PCHO matrix. This may be due to the changing clay amounts. According to the literature, the amount of clay in the polymer is an important parameter for the clay layers to be close to one another [13, 14]. These peaks mean partially exfoliated or intercalated structures in the polymer matrix. We can easily express that the high clay content can lead to uncompleted exfoliation and intercalated structures.

More information on the nanocomposite morphology is obtained by transmission electronic microscopy (TEM) observation as displayed in Figure 4 for nanocomposites. From the TEM images, it could be seen that exfoliated structures for low clay loading, intercalated, and stacked MMT platelets for high clay loadings were present in the polymer matrix. This structure may be described as the incomplete activation of diphenyliodonium group in the polymerization due to the limited mobility of these groups within the layers. It is generally observed that in case of higher clay loading, the amount of filler beyond the optimum limit leads to an increase of the filler-filler interaction instead of the more desirable filler-matrix interaction [15]. As a consequence of

Table 1: Thermal degradation temperatures of pure polymer and nanocomposites.

Sample	T_5 (°C)	T_{50} (°C)	T_{90} (°C)
PCHO	350	385	407
PCHO-M1	296	341	351
PCHO-M3	243	288	317
PCHO-M5	277	318	392

increasing these filler-filler interaction beyond the optimum limit, some stacking platelets could be formed in the polymer matrix [16]. The higher amount of the filler leading to agglomeration is observed in the nanocomposites as well. Moreover, nanoclays have the trend to form stacking platelets when their loading is beyond a certain level [17, 18].

Thermal stability of PCHO/clay nanocomposites and pure PCHO polymer was tested in nitrogen atmosphere and shown in Figure 5 and listed in Table 1. TGA results suggest the decomposition onset and mid-point degradation temperature of all nanocomposites decreased to lower temperatures with increasing clay content. This trend may be related to the catalytic activity of the clay on polymer decomposition process due to Brønsted and Lewis acid sites constituted by the clay lattice hydroxyl groups, which contact with the polymer matrix [19–21]. These sites in nanocomposite structure are responsible for the decreased thermal stability of the PCHO.

The char yields at 600°C were linearly increased for 0.25%, 0.5%, and 1% for clay loadings, respectively. This alteration of the char formation is attributed to the high heat resistance exerted by the clay itself [22]. The char residue of the hybrids at 600°C increased linearly because of the incorporation of the organoclay.

The glass transition is a complex phenomenon depending on a number of factors such as chain flexibility, molecular weight, branching, cross-linking, intermolecular interactions, and steric effects [23, 24]. The glass transition temperature of pristine PCHO is 62.3°C but it decreases with the addition of the clay for lower clay loading (Figure 6). The decrease trend in T_g by the addition of the nanoclay has also

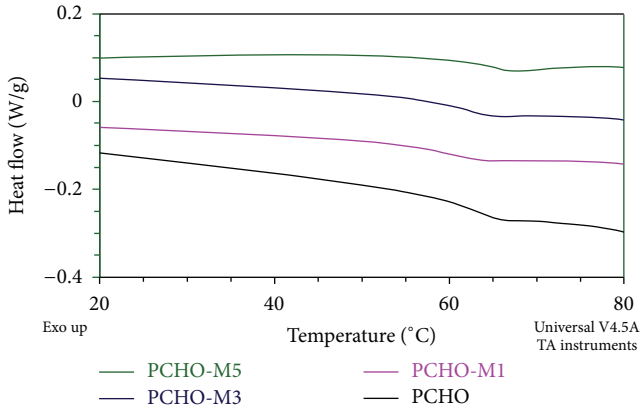

Figure 6: DSC data of pristine polymer and nanocomposites.

been observed by Lee et al. [25]. The intermolecular attractions of PCHO segments seem to be interrupted by the charged clay layers, and subsequently the PCHO backbone chains additionally gain the segmental mobility. It can also be addressed that the clay nanoparticles may provide steric factors that seemingly increase the chain flexibility of PCHO backbones. Conclusively, the MMT nanoclay imposes more flexibility and mobility to the PCHO backbones resulting in the decreased glass transition temperatures [23–25]. The amount of the nanoclay particles is large enough to provide steric effects that prevent the chains from packing compactly. This could increase the free volume of the polymer matrix and lead to the decrease in T_g [26].

The observed increase in the glass transition temperatures of these hybrids with the higher clay loadings could be the result of the restriction of the segmental relaxation of the chain segments near the clay layers. Similar results have also been obtained in other studies of polymer nanocomposites [27–29].

The molecular weight of this pure polymer was compared with the composites after the cleaving process. The effects of D-MMT on molecular weights of nanocomposites are shown in Table 2. It can be seen that the molecular weights increased for all clay loadings. Mn was changed from 8270 to 11232, 11839, and 12404 for pure PCHO and 1%, 3%, and 5% clay-loaded nanocomposites, respectively.

4. Conclusion

In conclusion, *in situ* photoinitiated polymerization of CHO through the intergalleries of clay was achieved by irradiating mixtures containing both photoinitiator and filler. The polymerization was shown to proceed via the cationic polymerization mechanism. Because of the propagating oxonium ions that were situated in the interlayer area of the clay layers, the polymerization was initiated in the interlayer area of the clay layers, and the exfoliated structures were attained. PCHO/clay nanocomposites were prepared with various clay loadings and characterized. The dispersion of silicate layers in the polymer matrix was confirmed by XRD and TEM measurements. Dispersions were found to be related to the amount of clay loading. TGA traces showed that the nanocomposites have lower thermal stabilities than those of the pristine PMMA. The char yields increased upon raising the clay content.

Table 2: GPC data of pure polymer and nanocomposites.

	Mn	PDI (Mw/Mn)	Conversation
PCHO	8270	1,670	85
PCHO/M-1	11232	1,498	93
PCHO/M-3	11839	1,540	80
PCHO/M-5	12404	1,412	76

The PCHO-montmorillonite nanocomposite was prepared via using bifunctional clay, which has both a catalyst and inorganic filler.

Acknowledgments

This research was supported by Çanakkale Onsekiz Mart University. The authors would like to thank Çanakkale Onsekiz Mart University for the financial support.

References

[1] E. P. Giannelis, "Polymer layered silicate nanocomposites," *Advanced Materials*, vol. 8, no. 1, pp. 29–35, 1996.

[2] G. Lagaly, "Introduction: from clay mineral-polymer interactions to clay mineral-polymer nanocomposites," *Applied Clay Science*, vol. 15, no. 1-2, pp. 1–9, 1999.

[3] A. Usuki, A. Koiwai, Y. Kojima et al., "Interaction of nylon-6 clay surface and mechanical-properties of nylon-6 clay hybrid," *Journal of Applied Polymer Science*, vol. 55, no. 1, pp. 119–123, 1995.

[4] K. Yano, A. Usuki, A. Okada, T. Kurauchi, and O. Kamigaito, "Synthesis and properties of polymide-clay hybrid," *Journal of Polymer Science A*, vol. 31, no. 10, pp. 2493–2498, 1993.

[5] P. C. Lebaron, Z. Wang, and T. J. Pinnavaia, "Polymer-layered silicate nanocomposites: an overview," *Applied Clay Science*, vol. 15, no. 1-2, pp. 11–29, 1999.

[6] M. Okamoto, "Recent advances in polymer/layered silicate nanocomposites: an overview from science to technology," *Materials Science and Technology*, vol. 22, no. 7, pp. 756–779, 2006.

[7] Z. Yenice, M. A. Tasdelen, A. Oral, C. Guler, and Y. Yagci, "Poly(styrene-b-tetrahydrofuran)/clay nanocomposites by mechanistic transformation," *Journal of Polymer Science A*, vol. 47, no. 8, pp. 2190–2197, 2009.

[8] A. Oral, M. A. Tasdelen, A. L. Demirel, and Y. Yaghi, "Poly(cyclohexene oxide)/clay nanocomposites by photoinitiated cationic polymerization via activated monomer mechanism," *Journal of Polymer Science A*, vol. 47, no. 20, pp. 5328–5335, 2009.

[9] P. Jackson, *Paint Resin Times*, 2002.

[10] J. P. Fouassier, *Photoinitiation, Photopolymerization, and Photocuring Fundamentals and Applications*, Hanser, Munich, Germany, 1995.

[11] J. V. Crivello, "Cationic polymerization—iodonium and sulfonium salt photoinitiators," *Advances in Polymer Science*, vol. 62, pp. 1–48, 1984.

[12] C. D. Shackelford, C. H. Benson, T. Katsumi, T. B. Edil, and L. Lin, "Evaluating the hydraulic conductivity of GCLs permeated with non-standard liquids," *Geotextiles and Geomembranes*, vol. 18, no. 2–4, pp. 133–161, 2000.

[13] S. S. Ray and M. Okamoto, "Polymer/layered silicate nanocomposites: a review from preparation to processing," *Progress in Polymer Science*, vol. 28, no. 11, pp. 1539–1641, 2003.

[14] A. Oral, M. A. Tasdelen, A. L. Demirel, and Y. Yagci, "Poly(methyl methacrylate)/clay nanocomposites by photoinitiated free radical polymerization using intercalated monomer," *Polymer*, vol. 50, no. 16, pp. 3905–3910, 2009.

[15] A. R. Azura, S. Ghazali, and M. Mariatti, "Effects of the filler loading and aging time on the mechanical and electrical conductivity properties of carbon black filled natural rubber," *Journal of Applied Polymer Science*, vol. 110, no. 2, pp. 747–752, 2008.

[16] H. Ismail, M. N. Nasaruddin, and H. D. Rozman, "The effect of multifunctional additive in white rice husk ash filled natural rubber compounds," *European Polymer Journal*, vol. 35, no. 8, pp. 1429–1437, 1999.

[17] A. Yasmin, J. L. Abot, and I. M. Daniel, "Processing of clay/epoxy nanocomposites by shear mixing," *Scripta Materialia*, vol. 49, no. 1, pp. 81–86, 2003.

[18] C. K. Lam, H. Y. Cheung, K. T. Lau, L. M. Zhou, M. W. Ho, and D. Hui, "Cluster size effect in hardness of nanoclay/epoxy composites," *Composites B*, vol. 36, no. 3, pp. 263–269, 2005.

[19] F. Bellucci, G. Camino, A. Frache, and A. Sarra, "Catalytic charring-volatilization competition in organoclay nanocomposites," *Polymer Degradation and Stability*, vol. 92, no. 3, pp. 425–436, 2007.

[20] G. Camino, G. Tartaglione, A. Frache, C. Manferti, and G. Costa, "Thermal and combustion behaviour of layered silicate-epoxy nanocomposites," *Polymer Degradation and Stability*, vol. 90, no. 2, pp. 354–362, 2005.

[21] K. Hiltunen, J. V. Seppälä, and M. Härkönen, "Effect of catalyst and polymerization conditions on the preparation of low molecular weight lactic acid polymers," *Macromolecules*, vol. 30, no. 3, pp. 373–379, 1997.

[22] J. H. Chang and Y. U. An, "Nanocomposites of polyurethane with various organoclays: thermomechanical properties, morphology, and gas permeability," *Journal of Polymer Science B*, vol. 40, no. 7, pp. 670–677, 2002.

[23] J. M. G. Cowie, *Polymers: Chemistry & Physics of Modern Materials*, edited by J. M. G. Cowie and V. Arrighi, Chapman & Hall, New York, NY, USA, 1991.

[24] R. H. Burton, M. J. Folkes, D. W. Clegg, and A. A. Collyer, *Mechanical Properties of Reinforced Thermoplastics*, edited by A. A. Collyer and D.W. Clegg, Elsevier, London, UK, 1986.

[25] J. H. Lee, T. G. Park, H. S. Park et al., "Thermal and mechanical characteristics of poly(L-lactic acid) nanocomposite scaffold," *Biomaterials*, vol. 24, no. 16, pp. 2773–2778, 2003.

[26] P. Krishnamachari, J. Zhang, J. Lou, J. Yan, and L. Uitenham, "Biodegradable poly(lactic acid)/clay nanocomposites by melt intercalation: a study of morphological, thermal, and mechanical properties," *International Journal of Polymer Analysis and Characterization*, vol. 14, no. 4, pp. 336–350, 2009.

[27] T. Agag and T. Takeichi, "Polybenzoxazine-montmorillonite hybrid nanocomposites: synthesis and characterization," *Polymer*, vol. 41, no. 19, pp. 7083–7090, 2000.

[28] F. M. Li, J. J. Ge, P. S. Honigfort et al., "Dianhydride architectural effects on the relaxation behaviors and thermal and optical properties of organo-soluble aromatic polyimide films," *Polymer*, vol. 40, no. 18, pp. 4987–5002, 1999.

[29] J. H. Chang, "Comparison of thermomechanical properties and morphologies of polyester nanocomposite fibers: PBT, PET, and PTT," *Polymer—Plastics Technology and Engineering*, vol. 47, no. 8, pp. 791–801, 2008.

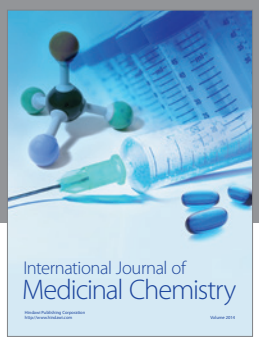

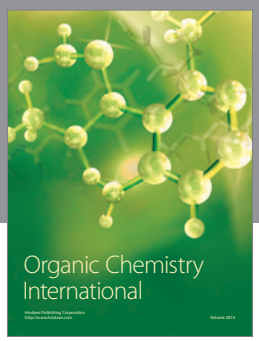

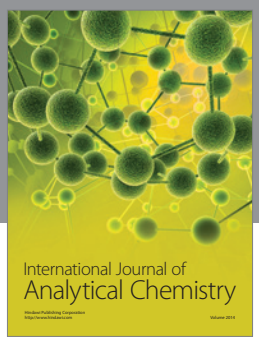

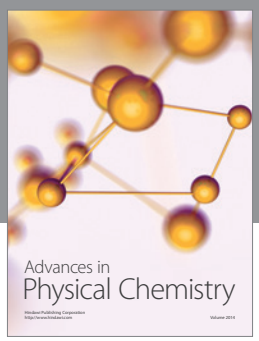

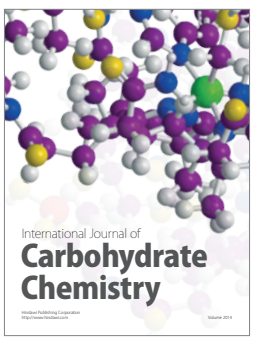

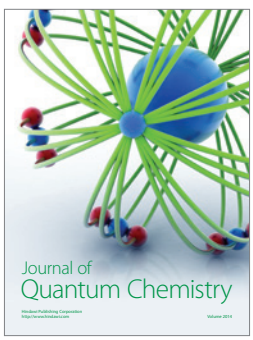

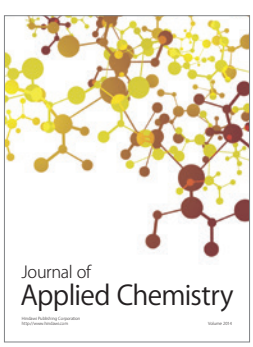

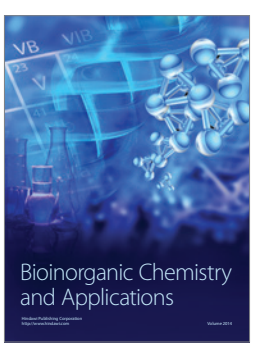

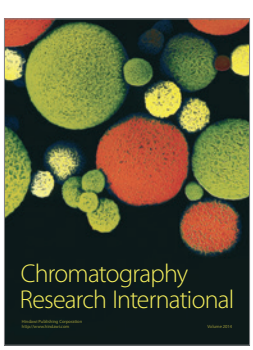

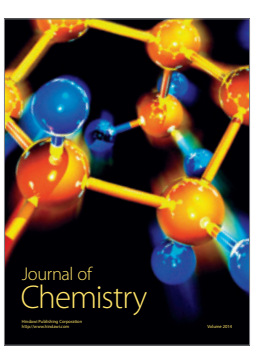

Hindawi

Submit your manuscripts at
http://www.hindawi.com